GIS-Based Geologic Mapping and Analysis of the Kaipo Mélange and southern Alpine Fault, New Zealand

Andre M. Mere, Nicolas C. Barth
University of California, Riverside

A combined approach utilizing airborne LiDAR data, in-person digital geologic field mapping, and GIS-based remote analysis allows for a new large-scale geologic map of the Kaipo Mélange and revised quaternary strike-slip rates for the southern Alpine Fault, New Zealand. We document a 1.5 x 3.5 km wide fault-parallel region of distributed quaternary active faulting and tectonic mixing of basement units related to progressive Australian-Pacific Plate boundary strain accumulation. We revise previously estimated southern Alpine Fault slip rates based on offset measurements of displaced glacial valley walls through identification and linear trend interpolation of well-preserved surfaces into the Alpine Fault trace. Our mean corrected offset measurement of 499.9 (+/- 28.9) m yields a Quaternary strike-slip rate of 27.7 (+2.8 / -2.6) mm/yr between the Hollyford Valley and John O'Groats River based on correlation to the timing of glacial retreat during the Last Glacial Maximum at 44°S in New Zealand. Our strike-slip rate is ~14% greater than previously published using the same offset glacial landforms.

INTRODUCTION

The South Island of New Zealand is divided along its length by the Australian-Pacific Plate boundary [Mortimer, 2017]. Through the South Island, the active plate boundary is represented by the 540km long right-lateral Alpine Fault, a structure analogous to the San Andreas Fault System, which has accommodated the majority of accumulated tectonic deformation since the Miocene (ca. 23 Ma), and records high quaternary slip rates presently thought to be distributed variably along strike [Norris & Cooper, 2001; Sutherland et al., 2006; Mortimer, 2014].

The Alpine Fault represents the single largest onshore seismic hazard in New Zealand, capable of producing a ≥Mw 8.0 earthquake resulting in significant property damage and even loss of life throughout much of the South Island [Sutherland, 2007]. Parameters including slip rate and fault zone material properties directly relate to capability and probability of rupture along the fault, and inform probabilistic earthquake forecasts used to inform public decision [Anderson et al., 1996; Field et al., 2013]. However, much of the Alpine Fault cuts through rugged topography and is covered by dense rainforest which poses difficulties for both access and field work.

Here, I use a combination of in-person digital geologic field mapping and proprietary 1m resolution airborne light detection and ranging (LiDAR) data to produce a new large-scale map of the Kaipo Mélange of Barth (2013) and I revise previous topographically derived slip-rate estimations through mathematical interpolation and measurement of offset glaci al landforms.

METHODS

In-person digital field mapping was conducted along the western Kaipo Valley flank, where several young multi-generational rotational landslides (e.g. the Kaipo Slips) expose bedrock units. Within older inactive landslide lobes, stream channels regularly feature steeply incised banks provided discontinuous bedrock exposure.

Correlation of units and structures was informed by a 1m grid-resolution Digital Terrain Model (DTM) and multi-hillshade raster derivatives of airborne LiDAR data. Airborne LiDAR has the capability of penetrating rainforest canopy to register ground returns, thus, geomorphic features that are difficult to visualize in the field or are unobservable in stereo-paired aerial photographs are comparatively simple to locate, interpret and measure using GIS software [Cowgill et al., 2012].

Alpine Fault strike-slip rates were investigated by identifying and projecting offset geomorphic markers into the fault plane [Zielke et al., 2014]. This method is a modernization and re-appraisal of slip rates presented by Sutherland (2006), which exploited ice-carved valley walls that formed continuous surfaces during the LGM, and were subsequently offset by Alpine Fault movement in the Holocene. Because glacially carved valleys display diagnostic U-shaped cross sections, a global second order polynomial was chosen for inexact interpolation of remnant elevation points not modified by fluvial and mass wasting processes.

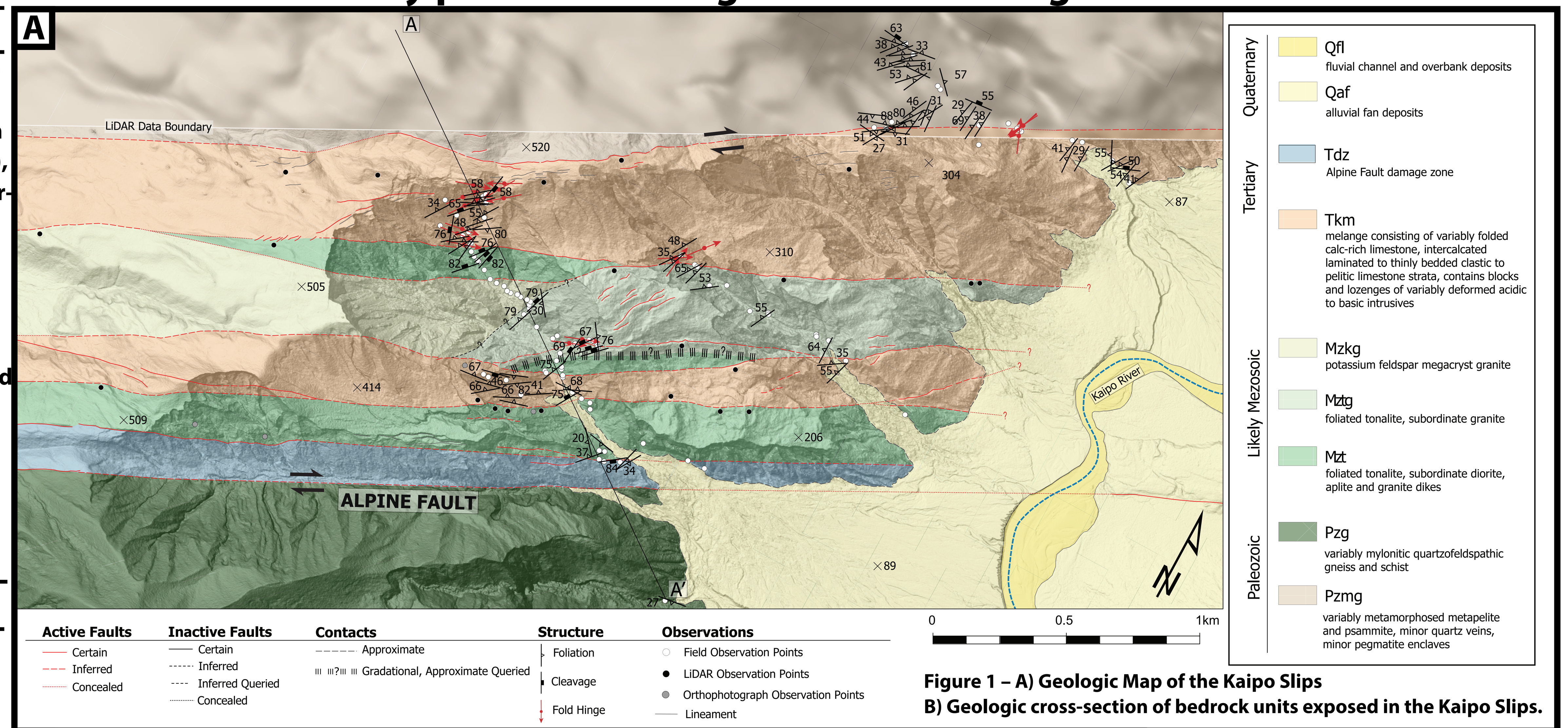

Figure 1 – A) Geologic Map of the Kaipo Slips
B) Geologic cross-section of bedrock units exposed in the Kaipo Slips.

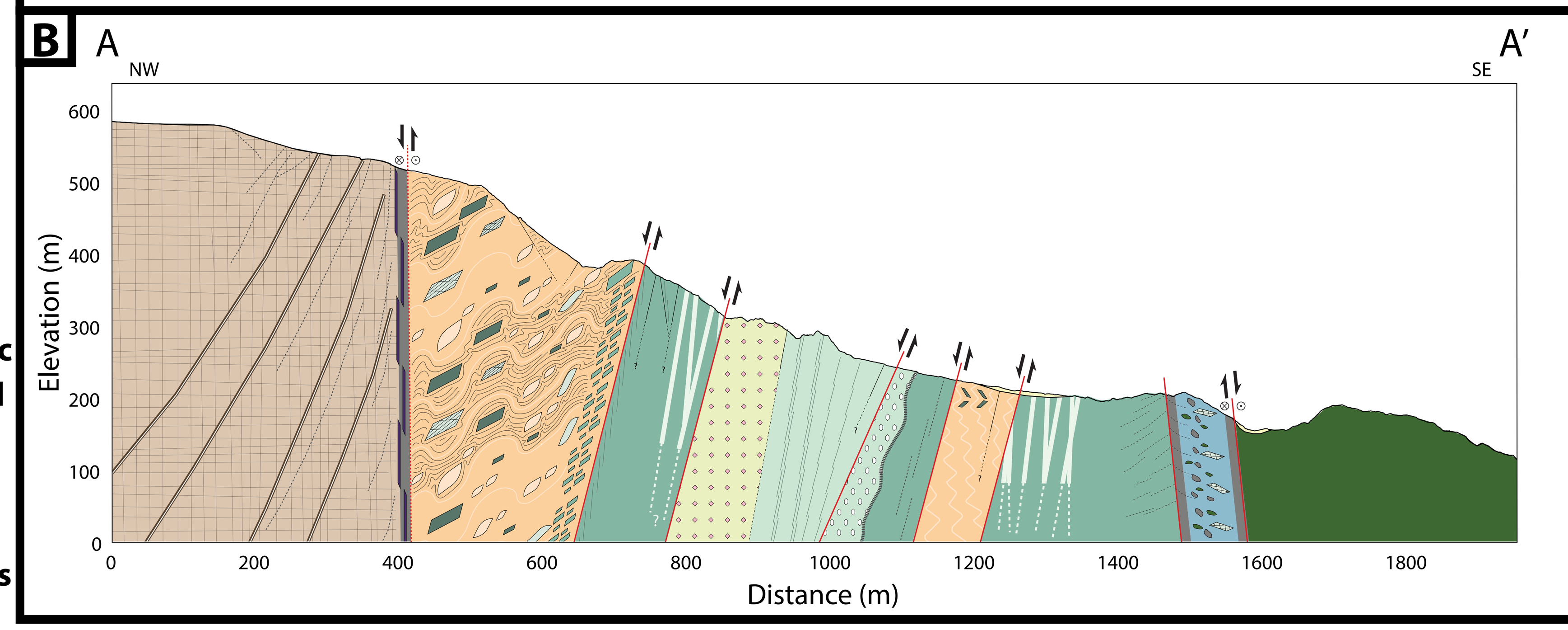

RESULTS

LiDAR data suggested the presence of multiple fault-line scarps that offset Tertiary cover sequences. Field investigation corroborated LiDAR interpretation, and resulted in the identification of additional associated fault splays and juxtaposed basement units [Figure 1A & B]. Field data indicate significant tectonic mixing of basement units within the Kaipo Mélange. The presence of multiple sizable fault-line scarps, widespread surface faulting, and possible repetition of in-faulted basement units indicate that upper crustal deformation related to plate boundary strain accumulation is more wide-spread than previously aknowledged in the Kaipo Valley [Figure 1A & B].

Interpolation of geomorphic surfaces resulted in contour patterns that generally appeared to correlate well across the fault plane at three of four locations. The interpolated contour pattern at Hollyford Valley does not appear to corrolate well. However, this offset location contains well preserved lateral moraines directly southeast of, and extending into, the Alpine Fault trace, as well as a potential lateral moraine crest assemblage further to the northwest [Figure 2A]. Thus, I choose to include offset measurements from the Hollyford Valley.

Offset measurements yielded a mean value of 499.9 (+/- 28.8) m at the 95% confidence level computed from Student's t-distribution [Table 1]. I opt to pool all offset measurements into one sample population based on the assumption that the abandonment ages of each glacially carved surface are statistically indistinguishable.

The timing of glacial abandonment in the study areas is inferred to correlate to at least the age of terminal moraines and recessional moraines at Lake Ohau, New Zealand. Thus, I use 10Be surface exposure ages of 18,220 (+/- 500) yr B.P. and 17,690 (+/- 350) yr B.P., corresponding to terminal and recessional moraine ages, respectively, as the maximum and minimum ages from which to derive slip rates [Putnam et al., 2013].

The southern Alpine Fault quaternary slip rate is 27.7 (+2.8 / -2.6) mm/yr.

DISCUSSION

High-resolution topographic data allow for increased accuracy of geologic mapping, and can prove indispensable in heavily vegetated and rugged areas. In this study, LiDAR informed field work, allowed for identification of otherwise obscured geologic structures, aided remote completion of digital mapping, and constrained the sense of displacement across active faults.

When measuring offset geomorphic markers for slip rate determination, LiDAR data allowed for (1) validation of the n ature of each offset geomorphic marker, (2) linear trend interpolation of geomorphic surfaces, (3) accurate determination of the location and bearing of the fault trace.

Our calculated slip rate for the southern Alpine Fault is ~14% greater than those constructed from linear extrapolation of contours derived from stero-paired photographs [Sutherland et al., 2006]. Notably, the southern Alpine Fault slip rate calculated via offset topography in this study overlaps within the error bounds of the geologically determined slip rate of Barth (2014) which was investigated within a few kilometers of this study area. These results appear to imply that the long-regarded notion that the Alpine Fault strike-slip rate diminishes to the south may not be correct, and that direct age-control on offset geomorphic markers is prudent. Both the widespread extent of easily deformed basement units and ~14% greater slip rate illuminated herein should likely be accounted for in probabilistic forecasts of seismic hazard.

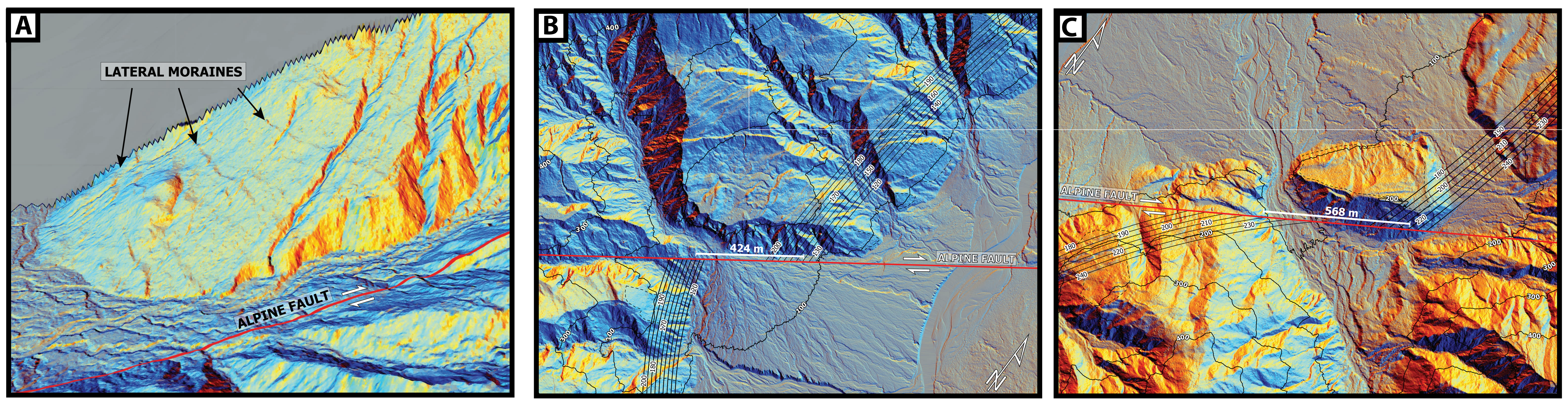

Figure 2 - A) Oblique view of multi-hillshade draped over DTM. Note preserved glacial landforms. B & C) Plane-view of Kaipo West and Kaipo E, respectivley. Thin black lines are equal elevation contours generated from linear trend interpolated glacial surfaces. Note the example measurement of equal elevation contour pairs.

HOLLYFORD		KAIPO EAST		KAIPO WEST		JOHN O'GROATS	
Contour (m)	Offset (m)	Contour (m)	Offset (m)	Contour (m)	Offset (m)	Contour (m)	Offset (m)
100	453	180	718	120	442	140	586
110	466	190	688	130	432	150	596
120	479	200	657	140	424	160	600
130	492	210	614	150	414	170	606
140	507	220	568	160	407	180	610
150	522	230	511	170	401	190	613
160	538	240	441	180	392	200	614
$\bar{x}$ = 499.9 m			s = 77.4 m		EBM = 28.9 m		

Table 1) Offset measurements of glacial valley wall offsets. Note that John O'Groats and Hollyford Valleys did not have suitable offsets preserved along the both valley walls.

REFERENCES CITED

Anderson, J. G., Wesnousky, S.G., Stirling, M.W.; Earthquake size as a function of fault slip rate. Bulletin of the Seismological Society of America ; 86 (3): 683–690.

Barth, N. C., C. J. Boulton, B. M. Carpenter, G. E. Batt, and V. G. Toy (2013), Slip localization on the southern Alpine Fault, New Zealand, Tectonics, 32, doi:10.1002/tect.20041.

Cowgill, E., Bernardin, T. S., Oskin, M. E., Bowles, C., Yıkılmaz, M. B., Kreylos, O., Elliott, A. J., Bishop, S., Gold, R. D., Morelan, A., Bawden, G. W., Hamann, B., Kellogg, L. H.; Interactive terrain visualization enables virtual field work during rapid scientific response to the 2010 Haiti earthquake. Geosphere ; 8 (4): 787–804. doi: https:/doi.org/10.1130/GES00687.1

Field, E.H., Biasi, G.P., Bird, P., Dawson, T.E., Felzer, K.R., Jackson, D.D., Johnson, K.M., Jordan, T.H., Madden, C., Michael, A.J., Milner, K.R., Page, M.T., Parsons, T., Powers, P.M., Shaw, B.E., Thatcher, W.R., Weldon, R.J., II, and Zeng, Y., 2013, Uniform California earthquake rupture forecast, version 3 (UCERF3)—The time-independent model: U.S. Geological Survey Open-File Report 2013–1165, 97 p., California Geological Survey Special Report 228, and Southern California Earthquake Center Publication 1792, http://pubs.usgs.gov/of/2013/1165/.

Mortimer, N. (2014), The oroclinal bend in the South Island, New Zealand, Journal of Structural Geology, Volume 64, 2014, Pages 32-38, ISSN 0191-8141, https://doi.org/10.1016/j jsg.2013.08.011.

Mortimer, N., Campbell, H. J., Tulloch, A. J., King, P. R., Stagpoole, V. M., Wood, R. A., Rattenbury, M. S., Sutherland, R., Adams, C. J., Collot, J. Seton, M. (2017), Zealandia: Earth's Hidden Continent, GSA Today, vol. 27, no 3, Mar. 2017

Norris, R. J., and A. F. Cooper (2001), Late Quaternary slip rates and slip partitioning on the Alpine fault, New Zealand, J. Struct. Geol, 23(2–3), 507–52 doi:10.1016/S0191-8141(00)00122-X.

Aaron E. Putnam, Joerg M. Schaefer, George H. Denton, David J.A. Barrell, Sean D. Birkel, Bjørn G. Andersen, Michael R. Kaplan, Robert C. Finkel, Roseanne Schwartz, Alice M. Doughty, The Last Glacial Maximum at 44°S documented by a 10Be moraine chronology at Lake Ohau, Southern Alps of New Zealand, Quaternary Science Reviews, Volume 62, 2013, Pages 114-141, ISSN 0277-3791, https://doi.org/10.1016/j.quascirev.2012.10.034.

Sutherland, R., Eberhart-Phillips, D.; Harris, R.A., Stern, T., Beavan, J., Ellis, S., Henrys, S., Cox, S., Norris, R.J.,, Berryman, K. R., Townend, J., Bannister, S., Pettinga, J., Leitner, B., Wallace, L., Little, T. A., Cooper, A. F., Yetton, M., Stirling, M. (2007); "Do Great Earthquakes Occur on the Alpine Fault in Central South Island, New Zealand?" A Continental Plate Boundary: Tectonics at South Island, New Zealand, American Geophysical Union (AGU), 2007, pp. 235–51. Wiley Online Library, doi:10.1029/175GM12.

Sutherland, Rupert, et al. (2006) "Quaternary Slip Rate and Geomorphology of the Alpine Fault: Implications for Kinematics and Seismic Hazard in Southwest New Zealand." GSA Bulletin, vol. 118, no. 3–4, Mar. 2006, pp. 464–74. pubs.geoscienceworld.org, doi:10.1130/B25627.1.

Zielke, O., Klinger, Y., Arrowsmith, R. J.; "Fault Slip and Earthquake Recurrence along Strike-Slip Faults — Contributions of High-Resolution Geomorphic Data." Tectonophysics, vol. 638, Jan. 2015, pp.43–62. ScienceDirect, doi:10.1016/j.tecto.2014.11.004.